

Magnetic properties of nanostructured ferromagnetic FeCuNbB alloys revealed by a novel method for evaluating complex Mössbauer spectra

This article has been downloaded from IOPscience. Please scroll down to see the full text article.

1999 J. Phys.: Condens. Matter 11 10545

(<http://iopscience.iop.org/0953-8984/11/50/340>)

View [the table of contents for this issue](#), or go to the [journal homepage](#) for more

Download details:

IP Address: 171.66.16.218

The article was downloaded on 15/05/2010 at 19:17

Please note that [terms and conditions apply](#).

Magnetic properties of nanostructured ferromagnetic FeCuNbB alloys revealed by a novel method for evaluating complex Mössbauer spectra

O Hupe†, M A Chuev‡, H Bremers†, J Hesse† and A M Afanas'ev‡

† Institut für Metallphysik und Nukleare Festkörperphysik, Technische Universität, Mendelssohnstrasse 3, 38106 Braunschweig, Germany

‡ Institute of Physics and Technology, Russian Academy of Sciences, Nakhimovskii avenue 36, 117218 Moscow, Russia

Received 21 July 1999, in final form 11 October 1999

Abstract. A novel method for analysing complex ^{57}Fe Mössbauer spectra has been successfully applied to nanostructured $\text{Fe}_{86-x}\text{Cu}_1\text{Nb}_x\text{B}_{13}$ ($x = 5, 7$). This method provides an objective model describing the measured spectra. This model consists of the largest meaningful number of lines, given by the 'quality' of the measured spectrum, i.e. by the criterion that all line parameters should be well defined. Using this method the temperature dependence of the mean hyperfine fields and the fractions of Fe atoms in different sites of the FeCuNbB samples are derived in the temperature range from 300 K to 700 K. In contrast to conventional methods for determining the hyperfine field distributions in magnetic alloys this approach allows us to evaluate the resulting hyperfine field distributions with indication of their mean-square deviations. The analysis results in detailed information about the iron nanograins, the amorphous residual phase and the so-called interface zone.

1. Introduction

Nanostructured alloys with soft magnetic properties are interesting for technical applications. Many investigations have been made to understand the magnetic properties of these alloys. They can be produced by the partial devitrification of amorphous alloys and consist structurally of nanosized crystalline grains with a long-range order and the residual amorphous matrix that exhibits short-range order. Mössbauer effect measurements on ^{57}Fe nuclei are an excellent tool for investigating iron-based nanostructured materials, because this local technique is able to elucidate the nature of hyperfine interactions of the different iron nuclei and to probe the nature of their immediate surroundings [1, 2]. Nevertheless the evaluation of such complex spectra is difficult because the models for their interpretation can be ambiguous.

Mössbauer spectra of magnetic alloys and amorphous materials consist usually of a great number of overlapping lines which are due to a variation of hyperfine parameters from site to site. In this case it is necessary to introduce continuous distributions of the hyperfine field, quadrupole splitting and isomer shift. Several methods have been proposed to resolve this problem [3–7]. The main advantage of these methods is that they do not require *a priori* information about the distribution shape. However, it is very difficult and sometimes impossible to extract quantitative information about partial contributions from different phases to the resulting distributions.

In the present paper we used a recently developed method for analysis of such complex Mössbauer spectra, which provides spectral models with the maximum meaningful number of lines and quantitative representation of a spectrum with well defined average values and dispersions of the parameters derived [8]. One of the basic concepts of this method is the 'densest possible solution' (DPS) which, for given Mössbauer source parameters, contains the maximum meaningful number of lines, while the χ^2 parameter of mean-square fitting is very close to unity. In some special cases, the DPS can be regarded as the final result of analysis [8] but, in general, the discrete forms found for the spectra can only approximate the real spectra in which continuous line distributions may exist along with discrete lines, just like the situation in nanostructured materials. As a rule, the shape of these distributions is unknown and must be analysed separately, but the most popular is a Gaussian one. The simplest way to test the presence of continuous distributions is to combine two closely spaced lines into a single line of a particular shape (e.g. the Voigt profile) whose width is an additional parameter. If the χ^2 value decreases as a result of this adjustment, the assumption that there is a continuous distribution is confirmed. The ideas mentioned above are realized within the computer program DISCOVER ('discrete versions of Mössbauer spectra') [8].

We have studied the $\text{Fe}_{86-x}\text{Cu}_1\text{Nb}_x\text{B}_{13}$ ($x = 5, 7$) alloys produced as amorphous ribbons. Isothermal annealing (1 h at 475 °C) lead to ultra-fine nanograins, embedded in the amorphous remainder. X-ray and electron scattering confirmed that these nanograins consist of bcc iron. The temperature dependence of magnetization and magnetic properties deliver information about the nanograins, the amorphous remaining phase and the interface phase. As the Curie temperature of the crystalline grains is much higher than that of the amorphous phase, the influence of this matrix can be investigated either for the ferromagnetic or paramagnetic state. In both cases the nanograins remain the same. The average grain-size (4 nm for Nb7 and 10 nm for Nb5), estimated from x-ray and electron diffraction measurements, is dependent on the niobium concentration and the annealing conditions [9].

Migliorini and coworkers [10–12] have investigated nanostructured materials similar to ours. In order to describe the Mössbauer spectra they used a spectral model which consists of two hyperfine field distributions (for amorphous and interface) and one discrete sextet (nanoparticles).

Migliorini *et al* used the information from the decomposition of the hyperfine field distribution to develop a model for the alloy topography. They distinguished four different iron sites:

- (i) Fe atoms in the bcc Fe nano grains;
- (ii) Fe atoms, structurally belonging to the nanograins, but situated on their surface;
- (iii) Fe atoms, situated in the amorphous remainder, but in close contact with the nanograins;
- (iv) Fe atoms in the amorphous matrix.

The Fe atoms assigned as (ii) and (iii) form the so-called interface.

In general there remains the problem of separating two or more distributions and estimating the region where they overlap. Our method for evaluating complex Mössbauer spectra within DISCOVER has its only restrictions in the statistical quality of the spectrum. A physically adequate model can be developed by an interactive process. So the model is not proposed in advance and tested during the evaluation, but will be developed during evaluation by regarding the quality of the description (χ^2 -value). To check the credibility of the model developed, a variation of external parameters, e.g. temperature, is necessary. Our preliminary results were published in [13].

2. Samples and experimental details

We have investigated the $\text{Fe}_{86-x}\text{Cu}_1\text{Nb}_x\text{B}_{13}$ ($x = 5, 7$) alloys, mentioned below as sample Nb5 and sample Nb7. The melt-spun amorphous ribbons (about $19 \mu\text{m}$ thick and $15 \text{ mm} \times 20 \text{ mm}$) were produced by the Vacuumschmelze GmbH Hanau, Germany. Isothermal annealing took place at 475°C for 1 h in a home made furnace under a protective He atmosphere. Investigations with electron microscopy showed that the samples consist of α -Fe-nanograins (about 4 nm in diameter for Nb7; 10 nm for Nb5), embedded in an amorphous remainder. To check the amorphous state of the as-quenched alloys, Mössbauer effect measurements were used. Annealing temperatures were estimated from differential scanning calorimetry (DSC) and magnetization measurements. For higher annealing temperatures FeB phases were observed as reported in [9]. The average grain size of the iron nanoparticles was estimated by electron diffraction and the Warren–Averbach method (x-ray).

For our Mössbauer investigations, a cosine-mode spectrometer with a ^{57}Co source in an Rh matrix was used in transmission geometry. The Mössbauer spectra were measured in the temperature range from 300 K to 700 K. Room-temperature Mössbauer spectra were recorded again after those performed at elevated temperatures to check the intactness of the initial state. The temperature measurements of Mössbauer spectra were performed in a home made furnace in vacuum ($p < 10^{-2}$ Pa) to prevent oxidation.

3. Analysis strategy of Mössbauer spectra within DISCOVER

At the first stage of analysis the DPS for a given spectrum is automatically found by the program DISCOVER. An example of such a solution for the Mössbauer spectrum of $\text{Fe}_{79}\text{Cu}_1\text{Nb}_7\text{B}_{13}$ taken at $T = 297 \text{ K}$ is presented in figure 1(a) which shows the DPS with 69 single lines with natural line width (after removing the influence of the finite absorber thickness and additional broadening in the source $\Delta\Gamma_s = 0.03 \text{ mm s}^{-1}$). It is clear that in this case, in spite of the very good description of the spectrum ($\chi^2 = 1.069$), all the lines in this spectral model are hardly possible to interpret which is quite natural for a sample where a distribution of parameters can be naturally expected. Therefore at the next stage of analysis we assume a variable Gaussian-type broadening of some lines (as a rule, the most intensive ones). Broadening of these lines during the fitting usually reduces the total number of lines (see figure 1(b): 44 lines with Gaussian broadening of the six most intensive lines). Such a description is considered to be adequate when χ^2 decreases or at least increases not too much. It is natural to suppose that the distributions observed at the previous stage of fitting describe first of all distributions of hyperfine fields in the ferromagnetic sample. That is why, as a next step of analysis, an extraction of magnetic sextets of lines is to be performed in order to obtain any real physical information.

The identification of sextets also begins usually with the most intensive pairs of lines which are the most probably expected outer lines of a magnetic sextet, that is followed by fitting with restrictions for the parameters of the corresponding lines (figure 1(c): 35 single lines and a sextet of Gaussian broadened lines). To simplify the evaluation of the spectra, the line intensities were fixed to the ratio 3:2:1:1:2:3 which is in accordance to the measurements. Such a step-by-step procedure results in describing the spectrum within a model with a number of sextets (with different line widths involved into the Voigt profiles) and some single lines which cannot be bound into sextets. These non-bound single lines may represent either any real sites of Mössbauer atoms in the sample or an imperfection of the model in the description of real distributions by the set of Gaussian lines. Generally speaking, such lines should be kept in the model if their removal highly increases χ^2 . A similar procedure can be used in order to

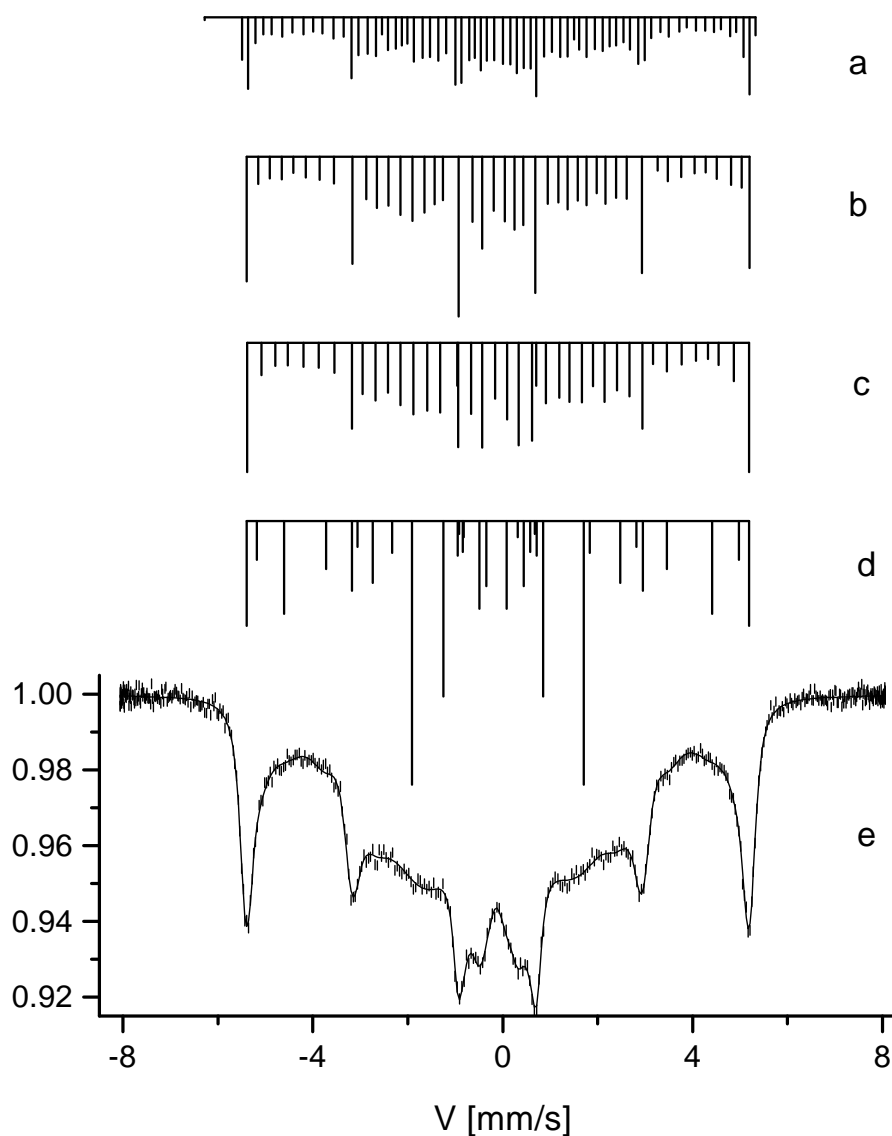


Figure 1. Room-temperature Mössbauer spectrum (e) of $\text{Fe}_{79}\text{Cu}_1\text{Nb}_7\text{B}_{13}$ and intermediate stages in the developing of the spectral model: (a) the 'densest possible solution' of 69 lines ($\chi^2 = 1.046$); (b) model of 44 lines and six Gaussian broadened most intensive lines ($\chi^2 = 1.069$); (c) model of 35 single lines and a sextet of Gaussian broadened lines ($\chi^2 = 1.072$); (d) the final model of five sextets and one doublet ($\chi^2 = 1.121$). The resulting spectrum calculated within the model (d) is shown in (e) as a solid line.

extract a quadrupole doublet among the remaining single lines (figure 1(d): five sextets and a quadrupole doublet of Gaussian broadened lines).

It is clear that the spectral model chosen should be matched for all the spectra of the same sample taken at different temperatures. So sometimes there is simply no other way to get physically adequate information but neglecting some 'undesirable' lines even if this gives an increase in the χ^2 value. One more specific feature inherent to the DISCOVER strategy is

that there may arise situations in fitting the spectra within a model chosen when parameters of some lines become hardly defined so that their mean square errors appear to be too large. For instance, such a situation occurs for the Mössbauer spectra taken at temperatures close to the Curie temperature of one of the magnetic phases so that the hyperfine structure corresponding to this phase collapses into a central line or a quadrupole doublet (see figure 2). In these cases the initial model is modified just within DISCOVER so that instead of the sextet a single line or a doublet is introduced into the current model. Correctness of this procedure is verified by the resulting χ^2 value.

As an example of the resulting models, figure 2 shows the experimental and calculated Mössbauer spectra of the sample Nb7, which are accompanied by partial contributions of magnetic sextets and a quadrupole doublet. As clearly seen from the figure, the spectra taken at different temperatures are well described within a self-consistent spectral model with rather low values of χ^2 , which is justified additionally by a spread of the corresponding residuals within the interval $[-3; 3]$ of the standard deviations.

Moreover, the approach realized within DISCOVER allows us to evaluate the resulting hyperfine field distributions in the following manner. Additional Gaussian broadening of lines of a magnetic sextet can be regarded as a good estimate for the distribution of the hyperfine field over different sites in the sample, which are represented by the sextet. Then, the total hyperfine field distribution for all ^{57}Fe atom sites in the sample can be expressed as a sum over all Gaussians used in the sextets in the model:

$$P(H_{hf}) = \sum_i \frac{A_i}{\sqrt{2\pi}\gamma_i} \exp\left[-\frac{(H_{hf} - \bar{H}_{hf}^{(i)})^2}{2\gamma_i^2}\right] \quad (1)$$

where A_i is the area of the i th sextet, γ_i is the additional Gaussian linewidth for the outer lines of the sextet and $\bar{H}_{hf}^{(i)}$ is the mean value of the i th hyperfine field. The corresponding distributions for the samples are shown on the right sides of figures 3 and 4. Due to the fact that the total hyperfine field distribution is determined in equation (1) by the parameters of lines which are adjustable in fitting, it is possible to estimate the mean square errors of $P(H_{hf})$ for each point H_{hf} as

$$\Delta P(H_{hf}) = \sqrt{\sum_j \sum_k \frac{\partial P(H_{hf})}{\partial p_j} \frac{\partial P(H_{hf})}{\partial p_k} (\Delta p_j \Delta p_k)} \quad (2)$$

where p_j are all the parameters involved in the definition (1), i.e. the areas, positions and Gaussian widths of lines for all the sextets; $(\Delta p_j \Delta p_k)$ are the elements of the covariance matrix which is calculated within fitting and accessible at any stage of the analysis within DISCOVER. The corresponding values of $\Delta P(H_{hf})$ restrict the resolution of the hyperfine field distribution evaluated with equation (1) and define a spread in $P(H_{hf})$ which is shown as dotted lines in figures 3 and 4. This circumstance predetermines an advantage of DISCOVER in obtaining the information about the hyperfine field distribution in comparison to the conventional methods for determining the hyperfine field distributions using smoothing restrictions [3–7] because within the last methods it is hardly possible to obtain information about the reliability of the distributions obtained.

4. Results and discussions

Following the procedure described above, the final spectral models of five sextets for both investigated samples have been obtained for the spectra taken below the Curie temperature for all the phases. The quadrupole doublet additional found for both the samples are due to some

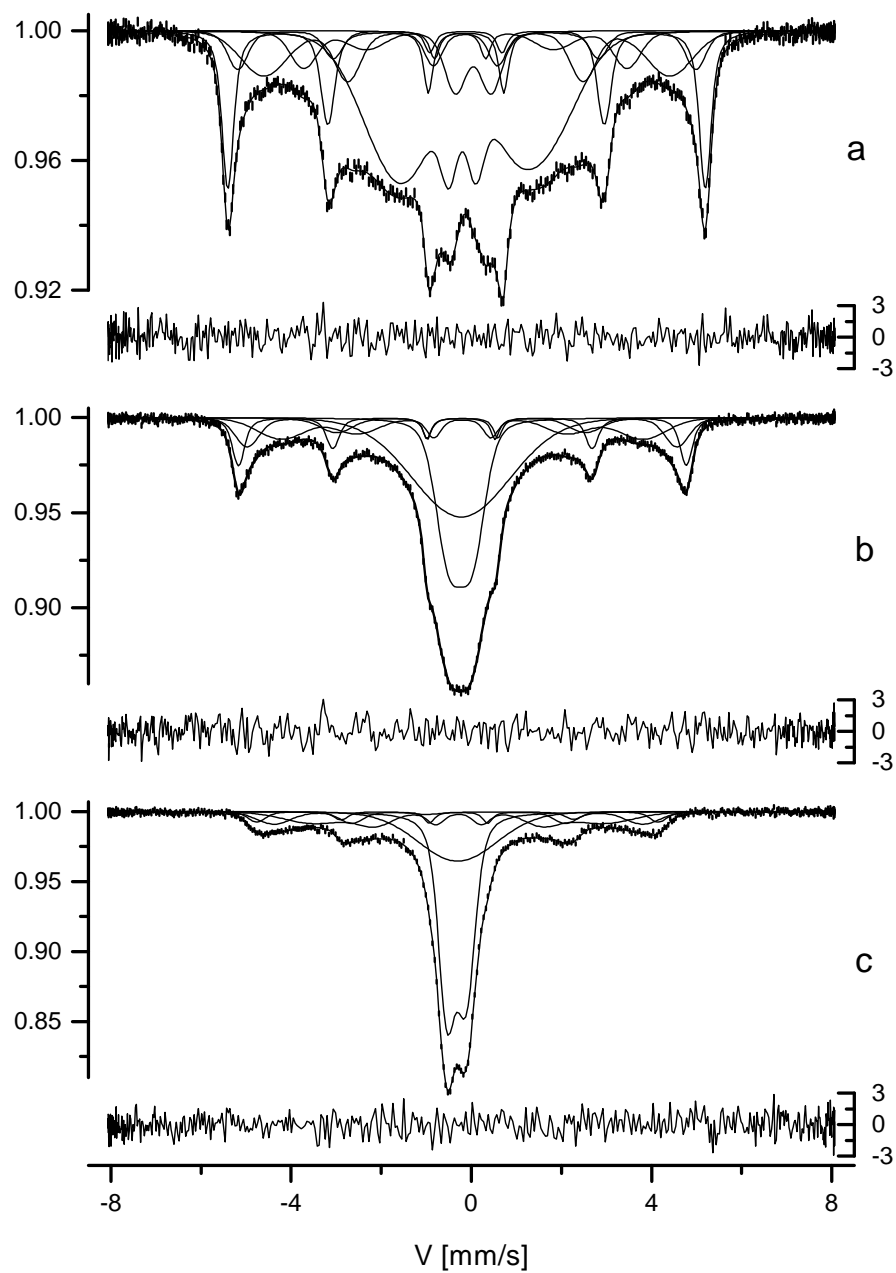


Figure 2. Mössbauer spectra of $\text{Fe}_{79}\text{Cu}_1\text{Nb}_7\text{B}_{13}$ taken at 297 K ($\chi^2 = 1.121$), 450 K ($\chi^2 = 0.931$), 600 K ($\chi^2 = 0.957$) (a)–(c) and corresponding calculated spectra and their partial components. Residuals in units of standard deviations are also shown below each spectrum.

paramagnetic contributions, belonging to the amorphous remainder and will not be discussed in detail here. It should be noted that the room-temperature spectrum for the sample Nb5 can be well described only in the model of six sextets, but in all the spectra taken at higher temperatures only five or fewer sextets could be resolved and below we will discuss only

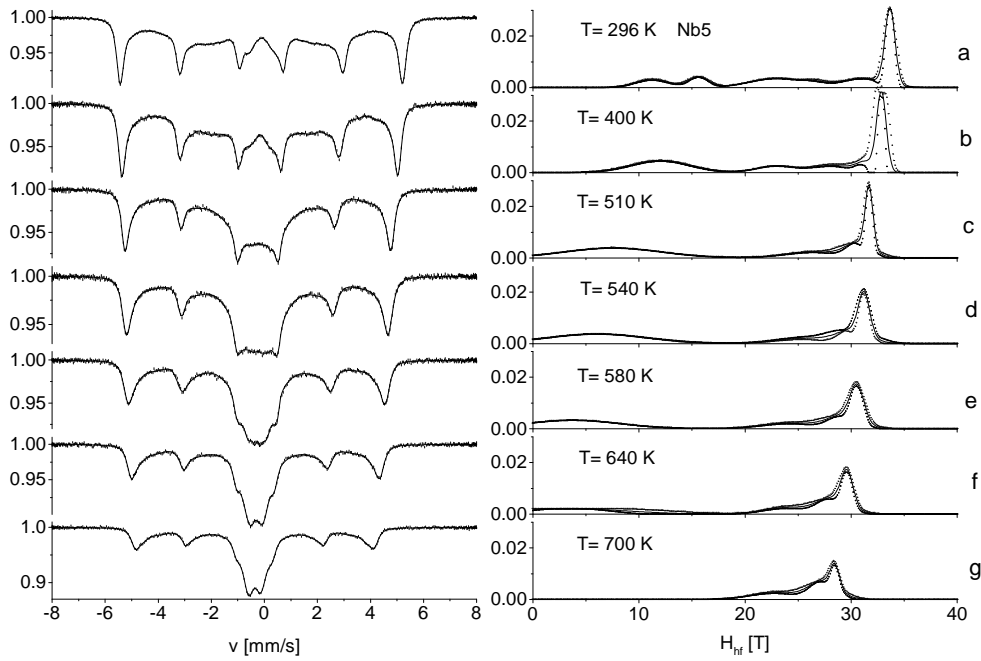


Figure 3. Mössbauer spectra (left) and corresponding hyperfine field distributions (right) for $\text{Fe}_{81}\text{Cu}_1\text{Nb}_5\text{B}_{13}$.

five contributions in the spectra for the sample Nb5. Figures 3 and 4 show the temperature dependence of the shape of Mössbauer spectra for our samples (left), together with their corresponding hyperfine field distributions $P(H_{hf})$ (right). The dotted lines in the figures represent the mean-square deviations $\Delta P(H_{hf})$ from the mean value $P(H_{hf})$. As clearly seen from the figures, the room-temperature spectra of both the samples are a superposition of sharp lines (with values of the hyperfine field of about 33 T) which can be associated with the crystalline (CR1) iron nanograins and a broad distribution from other different sites of Fe atoms in the samples.

The temperature dependences of the mean values of the hyperfine fields for different contributions into the spectra are shown in figure 5 where the curve for bcc Fe indicates the values measured for a foil of pure iron. As seen from figures 3–5, a similar temperature dependence of the hyperfine field distribution around sites CR1 in both the samples is observed up to 450 K; with temperature increasing the mean value of the hyperfine field decreases and the H_{hf} distribution becomes slightly broader. With further temperature increasing a monotonic behaviour of the hyperfine field distributions for the sites CR1 in the sample Nb5 remains, while for the sample Nb7 a broadening of the sharp lines with increasing temperature (also to be seen in the increasing width of the hyperfine field distribution) is observed. The latter can be explained by the distribution of the particles' Curie temperature and so the difference in the temperature dependence of the contributions CR1 in samples Nb5 and Nb7 can be associated with smaller grain size in the sample Nb7 (as has been confirmed by x-ray). Investigations to prove the presence of relaxation phenomena failed. The broadening of the lines is clearly determined to be of Gaussian shape and not Lorentzian. The DISCOVER program allows us to find out whether there is relaxation or not. If an additional Lorentzian line broadening is indicated by the program relaxation may be present.

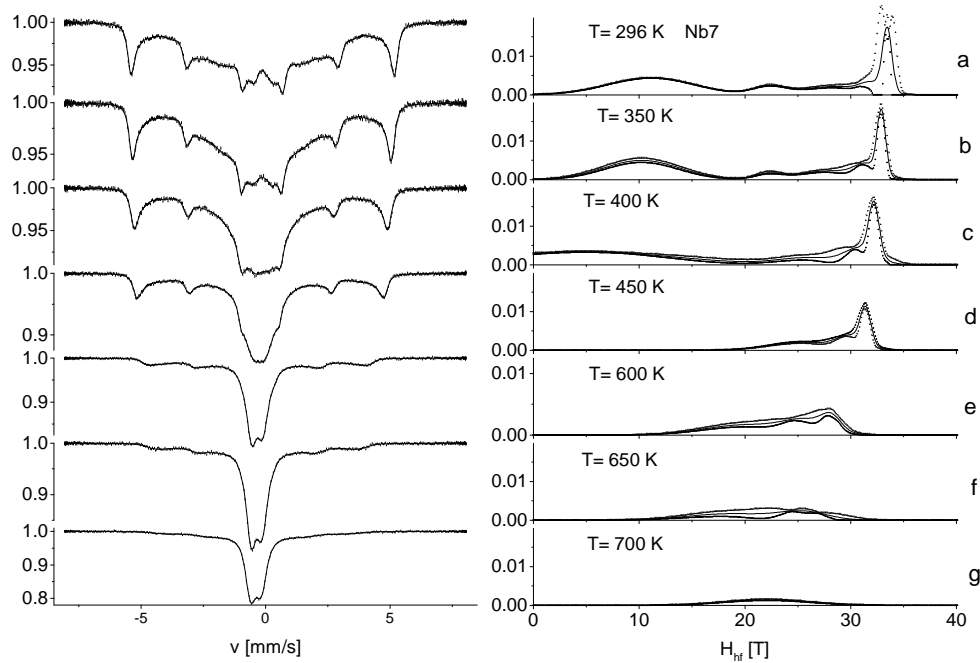


Figure 4. Mössbauer spectra (left) and corresponding hyperfine field distributions (right) for $\text{Fe}_{79}\text{Cu}_1\text{Nb}_7\text{B}_{13}$.

There is also a difference in the temperature dependence of the broad parts of the spectra for these two samples. The main difference between the room-temperature spectra is that the fraction of the broad part in the total spectral area for the sample Nb7 is essentially larger than that for the sample Nb5 (figure 6). One more sextet is necessary to describe well the spectrum of the sample Nb5, because more structure is seen in the spectrum.

An identification of the contributions into broadly distributed parts of the spectra can be done from the analysis of both hyperfine field distributions and mean values of the hyperfine fields as a function of temperature (figure 3–5). Because of the structural disorder, it is natural to attribute the broad distributions around values of $H_{hf} = 10\text{--}15\text{ T}$ and $20\text{--}25\text{ T}$ to the amorphous phases (AM1 and AM2, correspondingly). As far as the sample Nb7 is concerned, a rather monotonic temperature dependence of the contribution from the phase AM1 is observed with the Curie temperature $T_C \approx 410\text{ K}$ while the phase AM2 cannot be distinguished at temperatures higher than 350 K. The disappearance of this contribution is irreversible and can be explained by structural relaxation. (This contribution can only be found for the initial sample, which was not heated above 350 K. Dramatic changes in the sample can be excluded because of the similarity of the spectra with and without this contribution.)

Note that the T_C value for the phase AM1 is greater than $T_C = 350\text{ K}$ in the initial amorphous sample, which can be explained with different compositions after the annealing process. With temperature increasing above T_C for AM1 there are no traces of the hyperfine field distribution in the spectra of sample Nb7.

A qualitatively different behaviour is observed for the sample Nb5 (figure 5). First of all, there are two remaining contributions AM1 and AM2 which can be associated with the amorphous phase due to their lower values of hyperfine field and lower T_C . At higher temperatures, it is not possible to separate the AM1 and AM2 phases. The intensity of the

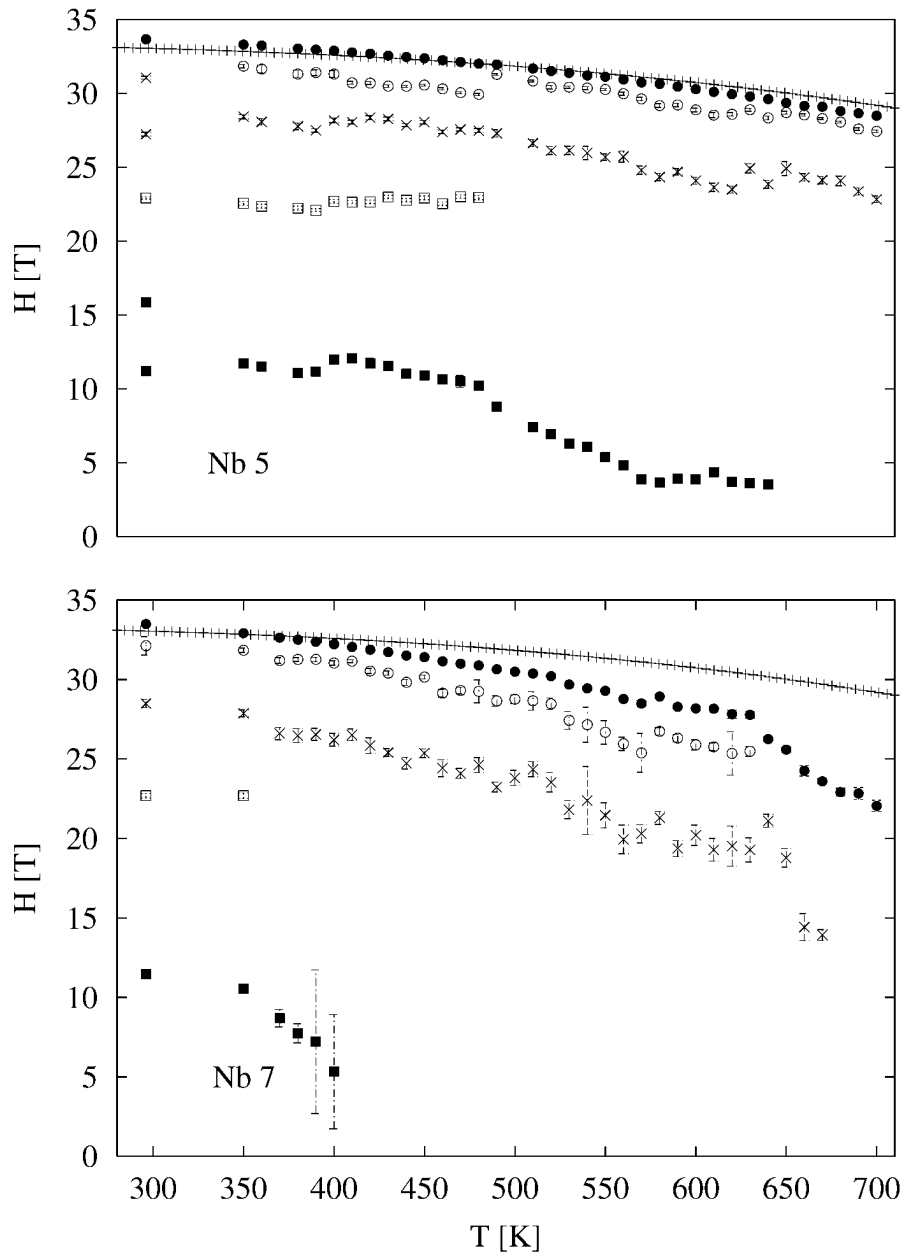


Figure 5. Temperature dependences of mean hyperfine fields for $\text{Fe}_{81}\text{Cu}_1\text{Nb}_5\text{B}_{13}$ (top) and $\text{Fe}_{79}\text{Cu}_1\text{Nb}_7\text{B}_{13}$ (bottom). Circles correspond to nanograins CR1 (closed) and CR2 (open), crosses to the interface IF, rectangles to the amorphous phase AM1 (closed) and AM2 (open), pluses to the bulk values of pure iron.

AM2 distribution is shifted to the AM1 distribution. The broadening of this distribution leads to the result that AM2 is disappearing at about $T_C \approx 470$ K in a very unconventional way (the mean value of hyperfine field remains up to the end but the relative fraction is decreasing). Proof for this interpretation is that the mean value of AM2 is slightly increasing instead of decreasing

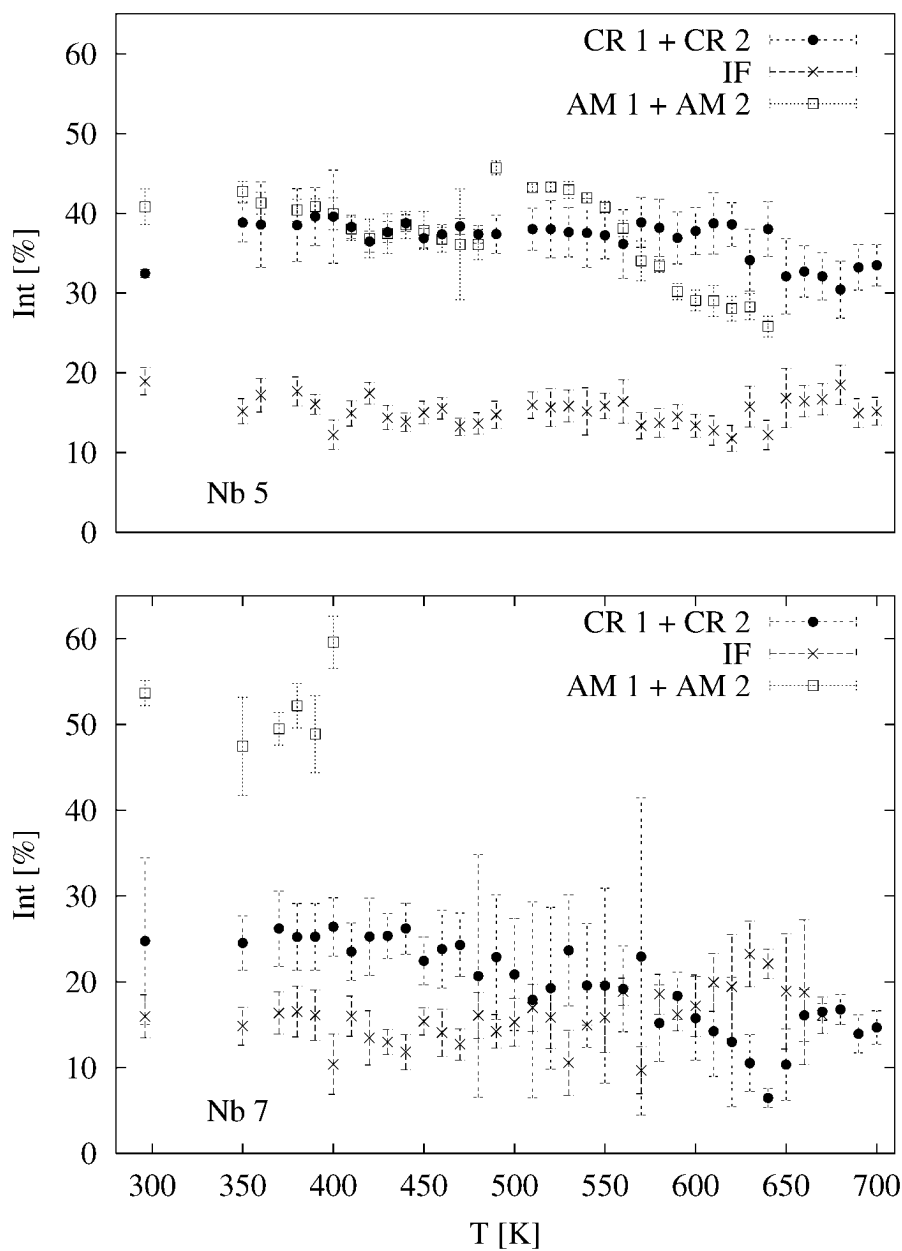


Figure 6. Partial areas of different magnetically split contributions to Mössbauer spectra against temperature for $\text{Fe}_{81}\text{Cu}_1\text{Nb}_5\text{B}_{13}$ (top) and $\text{Fe}_{79}\text{Cu}_1\text{Nb}_7\text{B}_{13}$ (bottom). CR1 and CR2 correspond to nanograins, IF to the interface, AM1 and AM2 to the amorphous remainder with the same markers as used in figure 5.

and that the total sum of both intensities remains. The plot (not shown) of the mean hyperfine field values (AM1 + AM2, values weighted with intensity) shows a conventional behaviour. In conclusion these two contributions are both associated with the amorphous phase and cannot be separated definitely. A monotonic temperature dependence of the contribution from the

phase AM1 is seen up to the higher temperature 650 K. Moreover, traces of the contribution as a very broad quadrupolar doublet remain up to the highest temperature 700 K and are directly seen even in the measured spectra. Besides that, a broad spread in the T_C value for this phase is observed in the temperature range from 550 K to 600 K. The Curie temperature of the initial amorphous sample was about $T_C = 430$ K, as determined by magnetization measurements.

As for the contribution with $H_{hf} = 25\text{--}30$ T at lower temperature, it is observed in the spectra of both the samples and demonstrates a rather high value of T_C . This contribution can be attributed to an interface phase (IF) which is magnetically coupled to the nanocrystalline iron (CR1) and not to the amorphous phase (AM1 and AM2), otherwise there would have had to be a kink in the curve at the Curie temperature of AM1. The hyperfine field of IF in sample Nb7 disappears at about 680 K. The contribution CR2 characterized by the values of H_{hf} very close to those of the CR1 phase can be interpreted as nano iron grains with impurities or perhaps as iron atoms on the surface of nanograins which would belong to the interface too, as proposed by Miglierini and coworkers [10, 11]. The evidence for an interface phase proposed by them is confirmed through our novel evaluation procedure.

For the sample Nb7 the contributions CR1 and CR2 could not be distinguished above 650 K (reversible process).

Such an interpretation is also justified by the temperature dependences of the partial spectral areas of different magnetically split contributions shown in figure 6. As seen from the figure, the fractions of the phases manifested in the spectra can be determined from their relative areas as ≈ 40 and 25% of CR, $\approx 16\%$ of IF, ≈ 45 and 59% of AM for the samples Nb5 and Nb7, correspondingly.

5. Conclusions

Using the DISCOVER method we have successfully analysed the complex ^{57}Fe Mössbauer spectra of nanostructured $\text{Fe}_{86-x}\text{Cu}_1\text{Nb}_x\text{B}_{13}$ ($x = 5, 7$) alloys. The temperature dependences of the mean hyperfine fields and the fractions of Fe atoms in different sites of the samples are derived in the temperature range from 300 K to 700 K. The analysis results in detailed information about the iron nanograins, the amorphous residual phase and the so-called interface zone.

Acknowledgments

We are grateful to the 'Internationales Büro des BMBF', Bonn, and the Russian Ministry of Science and Technology, Moscow, for supporting our collaboration within the project RUS-157-97. We also thank Dr G Herzer for the amorphous samples and Dr E Woldt for the DSC measurements.

References

- [1] Herr U, Jing J, Birringer R, Gonser U and Gleiter H 1987 *Appl.Phys.Lett.* **50** 472
- [2] Gonser U 1994 *Hyperfine Interact.* **94** 2261
- [3] Hesse J and Rübartsch H 1974 *J. Phys. E: Sci. Instrum.* **7** 526
- [4] Mangin P, Marshal S, Piecuch M and Janot C 1976 *J. Phys. E: Sci. Instrum.* **9** 1101
- [5] Le Caer G and Dubois J M 1979 *J. Phys. E: Sci. Instrum.* **12** 1083
- [6] Wivel C and Morup S 1981 *J. Phys. E: Sci. Instrum.* **14** 605
- [7] Brand R A and Le Caer G 1988 *Nucl. Instrum. Methods B* **34** 272
- [8] Afanas'ev A M and Chuev M A 1995 *JETP* **80** 560

- [9] Girhardt T, Friedrichs B, Woldt E, Hesse J, Efthimiadis K G and Chadjivasiliou S C 1999 *Nanostruct. Mater.* **12** 585
- [10] Miglierini M and Greneche J-M 1997 *J. Phys.: Condens. Matter* **9** 2303
- [11] Greneche J-M and Slawska-Waniewska A 1997 *Mater. Sci. Eng. A* **226–228** 526
- [12] Miglierini M, Labaye Y, Randrianantoandro N and Greneche J-M 1997 *Mater. Sci. Eng. A* **226–228** 559
- [13] Hupe O, Bremers H, Hesse J, Afanas'ev A M and Chuev M A 1999 *Nanostruct. Mater.* **12** 581